JOURNAL OF PROPULSION AND POWER
Vol. 26, No. 4, July–August 2010

Technical Notes

Turboprop Cycle Optimization Using Repulsive Particle Swarm Algorithm

Tayeb Boulkeraa* and Adel Ghenaiet†
Bordj el Bahri 16111 Algiers, Algeria

DOI: 10.2514/1.46491

Nomenclature

C	=	work output coefficient
Cp	=	specific heat, kJ/kgK
e	=	polytropic efficiency
F	=	objective function
f	=	fuel-to-air ratio
$g(X)$	=	inequality constraint
$\dot{m}$	=	mass flow, kg/s
H	=	altitude, m
Lcv	=	fuel heating value, kJ/kg
M	=	Mach number
P	=	pressure, Pa
T	=	temperature, K
V	=	speed, m/s
Wsp	=	specific power, kW/(kg/s)
X	=	design variables
γ	=	isentropic index
η	=	isentropic efficiency
ϑ_r	=	throttle ratio
π	=	total pressure ratio
τ	=	total temperature ratio

Subscripts

C, c	=	compressor, core
Cr	=	cruise
d	=	diffuser
f	=	fuel
g	=	gear
H	=	high pressure
L	=	low pressure
m	=	mechanical
n	=	nozzle
prop	=	propeller
r	=	ram
T	=	turbine
t	=	total
To	=	takeoff

I. Introduction

TURBOPROPS stay strong candidates for any application where high thrust and low fuel consumption are required. Compared with an equivalent technology turbofan, a turboprop will always enjoy the propulsion efficiency advantage at low speed and altitude, generally favoring advanced turboprops [1]. These latter have known evolutionary growth characterized by improvements in both specific power and fuel consumption. The T56 turboprop is a good example that has undergone a spectacular growth in which turbine temperature has increased about 190°F, requiring incorporating air-cooling [2]. When considering the design of a turboprop for an appropriate flight mission, the objective is to determine the optimum cycle parameters in terms of turbine inlet temperature (TIT), overall pressure ratio (OPR) and separate pressure ratios, and power turbine temperature expansion rate (TTR) corresponding to most of the extracted power with a residual jet thrust (5–10 % [3]), as well as engines' components technology level.

Many studies were undertaken by several authors to determine the turboprop's optimum cycle parameters, as an example, the PW100 turboprop [4] designed in cruise at 28,000 ft and 350 mph, has resulted in an OPR of 15 and a TIT of 2000°F. Brooks and Hirschkron [5] reviewed advanced turboprops for commuter aircraft and arrived at values of 17 and 2300°F. Hirschkron and Davis [6] carried out a study of advanced turboprops for a long endurance antisubmarine warfare (ASW) aircraft and proposed an OPR of 22 and a TIT of 2400°F for an engine in the 5000–6000 shaft horse power (SHP) class. Previous studies were based on extensive variations of parameters and involved only one objective usually fuel consumption, and did not show any comparison between performance of various turboprop designs under same operating conditions while considering the on-design and the off-design. In fact, the selection the best propulsion cycle and a configuration of a turboprop is intricate, due to many involved design parameters and constraints, hence optimization tools are inevitable for exploring the whole design space and producing feasible solutions for multiple objectives, generally conflicting and which can not be isolated from the mechanical design considerations. While high TITs are thermodynamically desirable, but need using expensive alloys and cooled blades leading to increased complexity and cost. The relatively small HP turbine blades could not use the same sophisticated cooling techniques as in large turbofans, so it would be necessary to operate at somewhat lower maximum cycle temperature [7]. On the other hand, higher OPRs must be considered in the issue of increased weight and engine complexity.

This paper presents a numerical approach to select an optimized turboprop engine configuration that matches with the power requirement of a class of propeller-driven aircraft. By adopting a biobjective [minimization of power specific fuel consumption (PSFC) and maximization of specific power Wsp] constrained optimization problem, the current design implies other criteria to be observed, and needed that the engine performance analyzer simulates both on-design and off-design operations. The optimizations used the repulsive particle swarm algorithm RPSO, which is a robust stochastic population-based algorithm, especially in solving nonlinear multimodal class of problems. The adopted multi-objective formulation is offering versatility in implementing a variety of operating conditions and taking in account the engine performance and technology constraints, and then offering possibilities to select the best configuration and its optimum design parameters. Such a methodology can be used in the preliminary design phase and in the course of design or as a decision aid when selecting an adequate motorization for this class of aircraft.

II. Turboprop Propulsion Cycle Modeling

Gas turbine engines can be modeled at various levels of details ranging from simple algebraic relations to full 3-D descriptions.

Received 26 July 2009; revision received 16 April 2010; accepted for publication 16 April 2010.

*Research Member, Laboratory of Thermal Power Systems, Applied Mechanics, EMP B.P. 17.

†Senior Lecturer, Laboratory of Thermal Power Systems, Applied Mechanics, EMP B.P. 17.

However, due to their low computational burden only simple aerothermodynamic models were considered in this contribution and implemented in this engine analyzer accommodating the preliminary designs. The three turboprops' configurations are shown in Fig. 1 illustrating different stations' numbering. The single-shaft fixed-turbine turboprop intended for a fixed speed operation has a simplified mechanical design, but penalties may result from the direct coupling between propeller and compressor. This has been overcome by the single-shaft free-turbine configuration offering the possibility to set the propeller speed independently from the gas generator. In the configuration of two-shaft fixed turbine, the low-pressure compressor is coupled to the propeller and variable stators are used to accommodate the variable propeller speed, hence alleviating penalties from propeller speed restrictions [7].

A. Parameter Derivation

We assume that the thermodynamic properties of the fluids depend on temperatures and fuel-to-air ratios. For a given fuel like JP8, many references give such relations [8]. The components losses and polytropic efficiencies for the basic and advanced technology turboprop correspond to the third and fourth technology level [9], noting that a technology level represents components performance in a 20-year period. The effect of cooling on turbine efficiency is accounted for by a reduction in polytropic efficiency and a correction in expansion ratio. The expansion from the exhaust nozzle is assumed nearly adiabatic and the turbine is unchoked.

The energy balance across the burner gives the fuel-to-air ratio as follows:

$$f = \frac{\tau_\lambda - \tau_C \tau_r \frac{Cp_{1,2}}{Cp_0}}{\frac{\eta_b Lcv}{Cp_0 T_0} - \tau_\lambda}, \qquad \tau_\lambda = \frac{Cp_4 T_{t4}}{Cp_0 T_0} \tag{1}$$

Single-shaft fixed turbine: the power balance between turbine, compressor and propeller yields

$$\frac{\dot{W}_{\text{prop}}}{\dot{m}_0 Cp_0 T_0} = \eta_g \left[\eta_m (1+f) \frac{Cp_{4,5}}{Cp_4} \tau_\lambda (1-\tau_T) + (1-\tau_C)\tau_r \frac{Cp_{2,3}}{Cp_0} \right] \tag{2a}$$

Expansion ratio: the expansion ratio as below is related to the temperature ratio by means of polytropic efficiency

$$\tau_T = 1 - \frac{Cp_4}{Cp_{4,5}} \frac{1}{\eta_m (1+f)\tau_\lambda} \left[\tau_r (\tau_c - 1) \frac{Cp_{2,3}}{Cp_0} + \frac{\dot{W}_{\text{prop}}}{\eta_g \dot{m}_0 Cp_0 T_0} \right] \tag{2b}$$

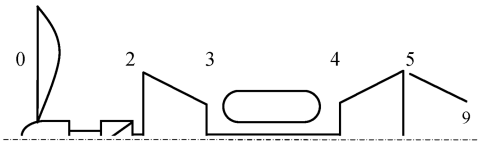

a) Single-shaft fixed-turbine

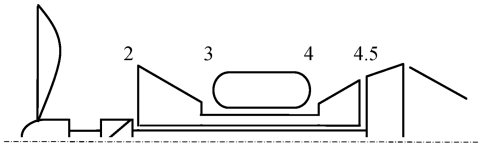

b) Single-shaft free turbine

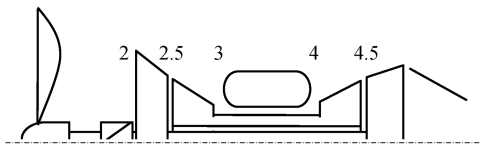

c) Twin-shaft fixed-turbine

Fig. 1 The configurations of three turboprops.

Single-shaft free-turbine: the output power from the free-turbine is used by the propeller

$$\frac{\dot{W}_{\text{prop}}}{\dot{m}_0 Cp_0 T_0} = \eta_g \eta_{mL} (1+f) \frac{Cp_{4.5,5}}{Cp_4} \tau_\lambda \tau_{TH} (1-\tau_{TL}) \tag{3a}$$

High-pressure (HP) turbine temperature expansion rate

$$\tau_{TH} = 1 - \frac{Cp_4}{Cp_{4,4.5}} \frac{Cp_{2,3}}{Cp_0} \frac{\tau_r (\tau_c - 1)}{\eta_{mH}(1+f)\tau_\lambda} \tag{3b}$$

Power turbine temperature expansion rate

$$\tau_{TL} = 1 - \frac{1}{\eta_g \eta_{mL}(1+f)\tau_\lambda \tau_{TH}} \frac{Cp_4}{Cp_{4.5,5}} \left[\frac{\dot{W}_{\text{prop}}}{\dot{m}_0 Cp_0 T_0} \right] \tag{3c}$$

Two-shaft fixed turbine: the turbine drives both low-pressure (LP) compressor and propeller

$$\frac{\dot{W}_{\text{prop}}}{\dot{m}_0 Cp_0 T_0} = \eta_g \left[\eta_m (1+f) \frac{Cp_{4.5,5}}{Cp_4} \tau_\lambda \tau_{TH} (1-\tau_{TL}) + (1-\tau_{CL})\tau_r \frac{Cp_{2,2.5}}{Cp_0} \right] \tag{4a}$$

HP turbine temperature expansion rate is as follows:

$$\tau_{TH} = 1 - \frac{Cp_4}{Cp_{4,4.5}} \frac{Cp_{2.5,3}}{Cp_0} \frac{\tau_r \tau_{CL} (\tau_{CH} - 1)}{\eta_{mH}(1+f)\tau_\lambda} \tag{4b}$$

LP turbine temperature expansion rate is given by

$$\tau_{TL} = 1 - \frac{Cp_4}{Cp_{4.5,5}} \frac{1}{\eta_{mL}(1+f)\tau_\lambda \tau_{TH}} \left[\tau_r (\tau_{CL} - 1) \frac{Cp_{2,2.5}}{Cp_0} + \frac{\dot{W}_{\text{prop}}}{\eta_g \dot{m}_0 Cp_0 T_0} \right] \tag{4c}$$

B. Engine Performance

For a turboprop engine it is more appropriate to consider the work supplied to the vehicle rather than the thrust, and to facilitate this, a dimensionless work output coefficient is used

$$C_{\text{tot}} = \frac{\eta_{\text{prop}} \dot{W}_{\text{prop}}}{\dot{m}_0 Cp_0 T_0} + \frac{F_c V_0}{\dot{m}_0 Cp_0 T_0} \tag{5}$$

The previous set of equations leads to a direct noniterative calculations of the thermodynamic parameters and engine performance:

1) Specific power is used to compare engines of various sizes as well as different types

$$W_{\text{sp}} = C_{\text{tot}} Cp_0 T_0 \tag{6}$$

2) PSFC is a ratio between the fuel flow and the power produced, which is inversely proportional to the overall engine efficiency

$$\text{PSFC} = \frac{f}{W_{\text{sp}}} \tag{7}$$

It is more usual when referring to a propeller-driven aircraft to consider the equivalent shaft horse power (ESHP) [3]

$$\text{ESHP} = \text{SHP} + \frac{FV_0}{\eta_{\text{prop}}} \tag{8}$$

When considering the off-design performance, the design variables are already known and the independent variables are basically the flight conditions and throttle settings. Off-design performance can be estimated without using the compressor and turbine maps based on a matching procedure between turbine and exhaust nozzle and a gas

generator matching. The effect of turbine rotational speed on mass flow and efficiency has been assumed to be of secondary nature due to the very restricted range of choked turbine. The throttle ratio $\vartheta_r = T_{t4\max}/T_{t4\text{sls}}$ is taken equal to 1.05 as same as the reference engine [10]. The conservation laws translate into a set of compatibility equations solved iteratively.

C. Single-Shaft Fixed Turbine

τ_C is computed iteratively using Eq. (2a)

$$\pi_T = k_2\sqrt{\tau_T}/\text{MFP}_9 \tag{9a}$$

$$\tau_T = 1 - \eta_T(1 - \pi_T^{(\gamma_{4.5}-1)/\gamma_{4.5}}) \tag{9b}$$

Single-shaft free turbine: The temperature drop in HP turbine is fixed, and then by using compatibility equations we have

$$\tau_C = 1 + k_1'\frac{\tau_\lambda}{\tau_r} \tag{10a}$$

$$\pi_{TL} = k_2'\sqrt{\tau_{TL}}/\text{MFP}_9 \tag{10b}$$

$$\tau_{TL} = 1 - \eta_{TL}(1 - \pi_{TL}^{(\gamma_{45-5}-1)/\gamma_{45-5}}) \tag{10c}$$

Two-shaft fixed turbine: similarly, we may obtain

$$\tau_{CH} = 1 + k_1''\frac{\tau_\lambda}{\tau_{CL}\tau_r} \tag{11a}$$

τ_{CL} is computed iteratively using Eq. (4a)

$$\pi = k_2''\sqrt{\tau_{TL}}/\text{MFP}_9 \tag{11b}$$

$$\tau_{TL} = 1 - \eta_{TL}(1 - \pi_{TL}^{(\gamma_{4.5-5}-1)/\gamma_{4.5-5}}) \tag{11c}$$

For each configuration, the mass flow is estimated by

$$\dot{m}_0 = k_0 p_0 \pi_r \pi_C/\sqrt{T_{t4}} \tag{12}$$

III. Optimization Procedure

The optimizations used the repulsive particle swarm algorithm RPSO, which is a robust stochastic population-based algorithm, especially in solving nonlinear multimodal class of problems. Such a technique performs searches both locally and globally, allowing a better exploration (group synergy) involving few parameters in addition to less CPU time compared with other evolutionary techniques. Particle Swarm algorithm PSO, originally developed by Kennedy and Eberhart in 1995 [11], is based on an evolutionary algorithm inspired by choreography of fish schooling and social-psychological theory. Every member of the swarm searches for the best in its surrounding and learns from its own experience. Moreover, each member learns from the others, typically from the best performer. Members of a swarm communicate good positions to each other and adjust their own position and velocity.

A. Repulsive Particle Swarm Method

The Particle Swarm method has many variants, such as repulsive particle swarm (RPS) method of optimization. Such variant is particularly effective in finding out the global optimum in very complex search spaces. Initialization is done with a population of random solutions (particles), and the recent velocity $v_{i+1}$of a particle is calculated by [12]

$$\begin{aligned} v_{i+1} &= \omega v_i + \alpha r_1(\hat{x}_i - x_i) + \omega\beta r_2(\hat{x}_{hi} - x_i) + \omega\gamma r_3 z \\ x_{i+1} &= x_i + v_{i+1} \end{aligned} \tag{13}$$

where x is the position and v is the velocity of the individual particle, r_1 and r_2 are random numbers $\in [0, 1]$, r_3 is a random number $\in [0, 1]$, z is a random velocity vector, $\hat{x}$ is the best position of a particle, and $\widehat{x}_h$ is the best position of a randomly chosen particle from within the swarm (instead of global best. $\alpha r_1(\hat{x}_i - x_i)$ is associated with cognition because it takes into account the particle's own experience, $\beta r_2(\hat{x}_{gi} - x_i)$ is associated with social interaction between the particles, α is called cognitive acceleration constant and β is called social acceleration constant, ω is inertia weight $\in [0.01, 0.7]$, and γ is a constant.

Occasionally, when the process is caught in a local optimum some chaotic perturbation in position, as well as velocity of some particle (s) may be needed. The traditional RPS gives little scope of local search to the particles, this why was modified by providing wider local search ability to each particle.

B. Constraints Handling

To guide the optimization process toward settings that ensure the must-meet performance requirements or constraints, such as the maximum permitted temperatures, the constraints' violations are penalized using an appropriate penalty function. Deb [13] developed a constraint handling method based on the penalty function approach. This penalization technique has the advantage that it does not use any extra parameter and considers both the population of solution at hand and the amount of constraint violation in the objective function calculations. Mathematically, the objective function is formulated as follows:

$$F(X) = \begin{cases} f(X) & \text{if } g_j(X) \geq 0 \\ f_{\max} + \sum_{j=1}^{\text{NCON}} |g_j(X)| & \text{otherwise} \end{cases} \tag{14}$$

The parameter$f_{\max}$ is the objective function values of the worst feasible solution in the population (swarm) and $g_j(X)$ are the constraints.

C. Application to Turboprop Engines

We intend to determine a set of optimum cycle parameters for three variants of turboprops matching with a propeller-driven aircraft operating in cruise flight at an altitude of 28,000 ft and Mach number of 0.475 [14]. Mission constraints analysis undertaken in a previous work has led to a takeoff minimum power of 4795 hp per engine. The operation and design constraints should be observed, in this instance, a design with a power less than that required at takeoff and cruise will not be acceptable. Also, there are constraints of compressor exit temperature not exceeding 750 K (for titanium blades) and LP turbine entry temperature not exceeding 1050 K for a basic technology level and 1250 K for an advanced technology level [15].

In this biobjective optimization tradeoffs are inevitable because it is practically impossible to find a single design satisfying all the conflicting objectives and constraints, thus we search for an efficient (noninferior, nondominated) solutions set, which is referred to as the best compromise solutions or optimal Pareto set [16,17]. Then, the decision maker can pick the proper compromise from these alternative solutions.

In our case study, the biobjective optimization problem of PSFC that has to be minimized and Wsp to be maximized is stated as follows:

1) Find design parameters $X = [\pi_{CH}, \pi_{CL}, T_{t4}, \tau_{TL}]^t$ that minimize $F = [\text{PSFC}^{-1}, W_{\text{sp}}]^t$.

2) Subject to the design limits and constraints given in Tables 1 and 2.

This biobjective formulation is reduced by using the weighted sum [17,18]. To enable aggregation of different objectives and constraints of different units and magnitudes in a single equation, the normalization is imperative to bring their values into the same scale. That means the numerical model of the engine must be capable of simulating engine performance at cruise flight at standard day (design point) and takeoff at hot day (off-design).

Table 1 Design variables space

Lower limit	Design variable	Upper limit
5	High pressure ratio	15
1.2	Low pressure ratio	2.5
7	Overall pressure ratio	25
0.4	Turbine temperature ratio	0.8
1150 K	Turbine inlet temperature (basic technology)	1205 K
1200 K	Turbine inlet temperature (advanced technology)	1700 K

Table 2 Design constraints

Design constraint	Basic technology limit	Advanced technology limit
T_{t3}, K	750	800
$T_{t4.5}$, K	1050	1250
$ESHP_{To}$, hp	4795	4795
$ESHP_{Cr}$, hp	2100	2100

IV. Results and Discussion

A. Models Validation

Tables 3 and 4 give validations based on the availability of data of two turboprops variants, the T56-15-A [10] (single-shaft fixed turbine) and PT6A-62 [19] (single-shaft free turbine), considering a throttle ratio equal to 1.05. It can be concluded that the results obtained by the present performance analyzer's modeling are acceptable. For the third turboprop configuration (no data is available to compare with) we assumed the validity of the modeling, since it is basically a combination of the two previous configurations. Based on these validations at design and off-design points the engines' moldings are felt that may be used in actual optimizations.

Table 3 Validation for the single-shaft fixed turbine with T56-15-A [10] takeoff performance $M = 0$ ISA conditions

Parameter	Predicted	Reference [10]	Error %
Turbine inlet temperature, K	-	1322	——
Overall pressure ratio	9.5	9.5	——
T_{t5}, K	756.3	741.5	2.0
m_c, kg	——	14.74	——
$ESHP_{To}$, hp	4996.4	4900.0	1.96
$PSFC_{To}$, lb/h/hp	0.525	0.515	1.9
Flight performance at $M = 0.475$ and $H = 28000$ ft			
Turbine inlet temperature, K	1205	1205	——
Overall pressure ratio	10.80	——	——
T_{t5}, K	691.5	——	——
m_c, kg	6.61	6.76	2.22
$ESHP_{Cr}$, hp	2066.42	2190.0	5.64
$PSFC_{Cr}$, lb/h/hp	0.452	0.445	1.6

Table 4 Validation for the single-shaft free-turbine with PT6A-62 [19]

Takeoff performance $M = 0$. TIT = 1269.5 K ISA conditions			
Parameter	Predicted	Reference [19]	Error %
$P_{t4}/P_{t4.5}$	3.1026	3.0420	2.0
$P_{t4.5}/P_{t5}$	2.5782	2.5109	2.7
T_{t3}, K	558.28	592.43	5.8
$T_{t4.5}$, K	1032.33	1000.04	3.2
T_{t5}, K	800.22	820.63	2.5
Power specific fuel consumption, kg/kW · h	0.3668	0.3658	0.27
Shaft horsepower, hp	979.0	950.0	3.0
Flight performance at $M = 0.2$ TIT = 1269.5 K and $H = 3048$ m			
m_c, kg/s	2.8703	2.8502	0.7
Overall pressure ratio	9.10	——	——
Power specific fuel consumption, kg/kW · h	0.3477	0.3420	1.7
Shaft horsepower, hp	837.46	749.88	11.7

B. Optimization Results

First, we performed a cycle optimization considering a basic technology level to determine the optimum TIT, OPR, and TTR and the subsequent performance for the three configurations of turboprops. Figure 2 shows the feasible domain and the tradeoffs surface (Pareto front) for the single-shaft fixed-turbine turboprop. According to the data of the reference turboprop T56-15-A, this latter at a TIT of 1205 K is producing an ESHP of about 2190 hp and a PSFC of 0.445 lb/hp/h. Thus, the reference design point is close to the Pareto front and constitutes an optimal design for which the manufacturer has given more importance to the power at takeoff for an engine to power a short landing and takeoff aircraft.

Optimization convergence history depicted in Figs. 3–5 show that the process converges in few iterations (about 30–40). Preliminary peaks are due to the chaotic perturbation in position as well as velocity of some particles imposed to make the exploration more efficient and avoid caught in local optimum. The particular convergence path of the objective function (Fig. 5) is evidence that the RPSO converges rapidly. The first steps (1–15) are due to search for the feasible solutions, and once these feasible solutions are found, the algorithm can actually perform to converge.

Figure 6 clearly show that TIT is at a maximum tolerated value, confirming that higher values are always favorable for both PSFC and Wsp. On the other hand, the optimum values of overall pressure ratio and turbine temperature expansion rate are varying considerably. Furthermore, it seems that the optimization is guided by the constraint of temperature at compressor exit which limited the Pareto front at point DP2, as seen from Fig. 7. All points on this front constitute an optimal design, but the final design points depend on other criteria, for instance if taking into account the maximum power at takeoff, the point DP1 constitutes a good choice. On the other side, design point DP2 is another choice for improving PSFC to increase flight range. For a compromise between performance and reliability, the nearest design point DP3 to the ideal one constitutes a good tradeoff for PSFC and Wsp and avoids working at the maximum constraints of temperatures. If one desires a greater power with a noticeable gain in PSFC, the size of the turboprop should be reconsidered. Table 5 gives the optimum cycle parameters and performance corresponding to the proposed design points.

The optimization computations of the two other configurations in the same conditions, keeping the same design criteria, have led to the results as seen in Figs. 8–11. By comparing the power at takeoff for the same cycle parameters, it is visible that the single-shaft fixed-turbine turboprop performs well; this is because $T_{t4.5}$ limit

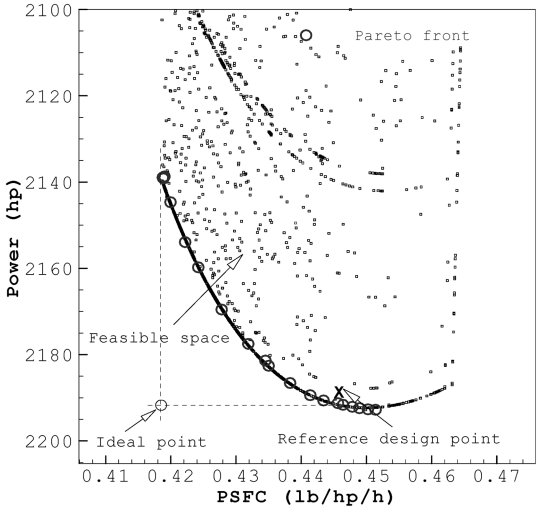

Fig. 2 Feasible domain and tradeoff surface (Pareto front) for a single-shaft fixed-turbine turboprop.

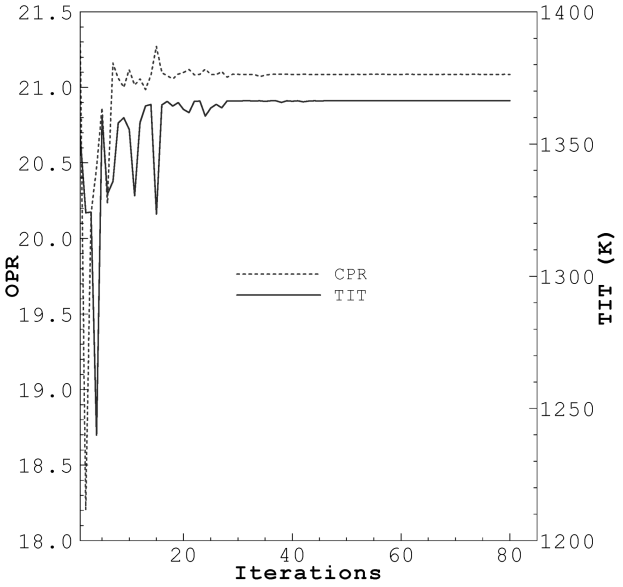

Fig. 3 Parameters' convergence history.

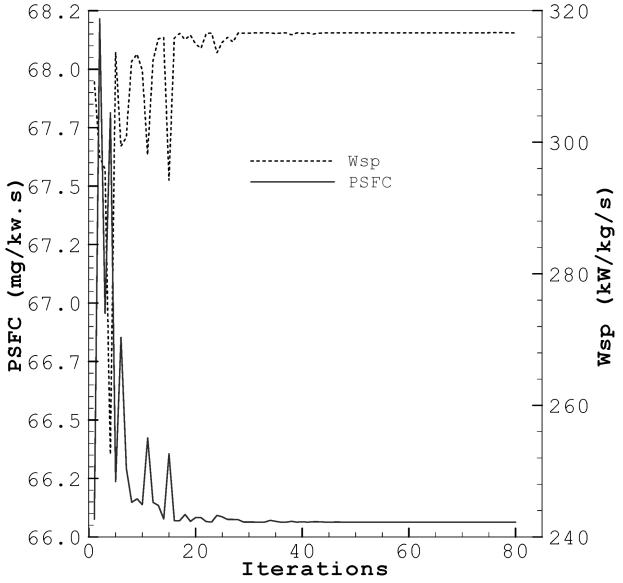

Fig. 4 Performance's convergence history.

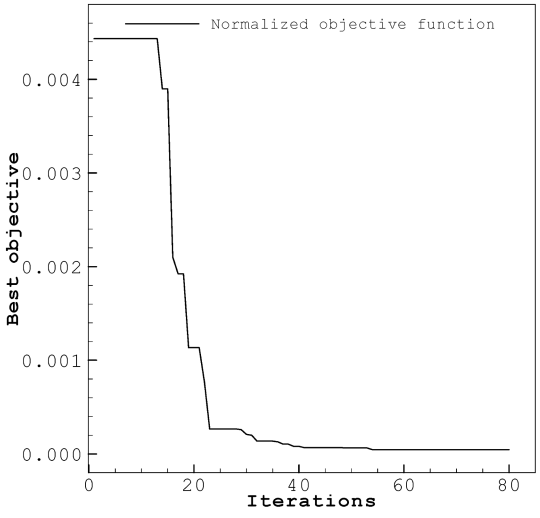

Fig. 5 Best particle's performance history.

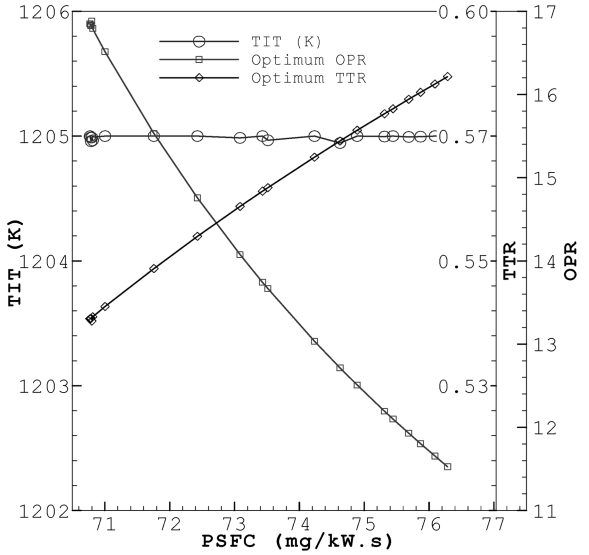

Fig. 6 Optimum cycle parameters for a single-shaft fixed-turbine turboprop.

(1050 K) for an uncooled LP turbine was too severe and became an active constraint that limited improving the power at takeoff. Also, TIT at cruise was at its maximum tolerated value of 1205 K. For this takeoff power range and a basic technology it seems that the single-shaft fixed turbine turboprop is a good performer. Figures 9 and 11 depict the proposed design points, which are also presented in Table 5.

As depicted in Fig. 12, the optimization process was guided for the two last versions by LP turbine entry temperature constraint $T_{t4.5} \leq$ 1050 K and by the constraint of power at takeoff ESHP $\leq$ 4795 hp which limited the maximum Wsp and PSFC, respectively. The compressor exit temperature T_{t3} constitutes a strong constraint and guided the optimization process only for a single-shaft fixed-turbine configuration, hence limited the minimum PSFC, whereas the improvement limit of Wsp was not due to constrains, but because Wsp was shown to drop when OPR is around 11.5.

We may conclude from these optimizations of turboprops' variants, considering a basic technology level and same operating conditions as the reference engine T56-A-15, that the optimum OPR is laying in between 11.53–17.60, hence resulting in Wsp ranging from 241.8 to 248.6 kW/kg/s and PSFC in between

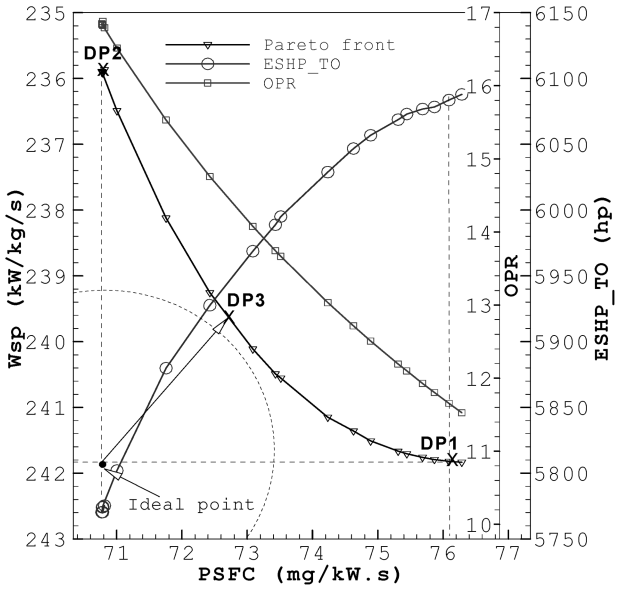

Fig. 7 Tradeoffs surface (Pareto front) for a single-shaft fixed-turbine turboprop.

Table 5 Optimum design parameters for a basic technology level

	Single-shaft fixed-turbine			Single-shaft free-turbine			Two-shaft fixed-turbine		
Design parameters	DP1	DP2	DP3	DP1	DP2	DP3	DP1	DP2	DP3
Overall pressure ratio	11.53	16.85	14.53	12.03	17.60	15.21	12.74	17.42	15.64
High pressure ratio	——	——	——	——	——	——	10.62	14.52	12.98
Low pressure ratio	——	——	——	——	——	——	1.20	1.20	1.205
Turbine inlet temperature, K	1205.0	1205.0	1205.0	1205.0	1200.0	1205.0	1205.0	1200.0	1205.0
Power turbine temperature ratio	0.5869	0.5388	0.5572	0.7302	0.7158	0.7196	0.7125	0.6994	0.7024
Design performance									
*W*sp, kW/kg/s	241.82	235.9	239.55	245.03	235.65	242.15	248.62	240.69	245.82
Power specific fuel consumption, mg/kW · s	76.09	70.77	72.64	74.52	69.28	70.97	72.40	68.10	69.36
Off-design performance									
Equivalent shaft horsepower at takeoff, hp	6083.58	5771.39	5943.19	4885.10	4795.0	4838.48	4823.26	4795.29	4795.10

76.09 – 68.10 mg/kW · s. According to Figs. 12 and 13 it seems that the third variant of two-shaft fixed-turbine turboprop gives better performance in cruise (dominant front) for the same TIT and OPR, however, the final design choice may be reconsidered with respect to other design criteria.

For an advanced technology level, keeping same operating conditions and throttle ratio, the explored space of design variables and constraints limits are given in Tables 1 and 2. Initially, optimizations were carried out for an OPR from 7 to 25, but for the two-shaft fixed-turbine version, Pareto fronts have practically

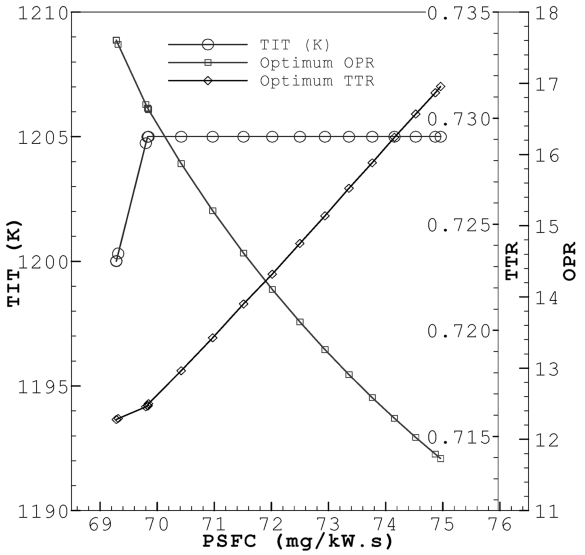

Fig. 8 Optimum cycle parameters for a single-shaft free-turbine turboprop.

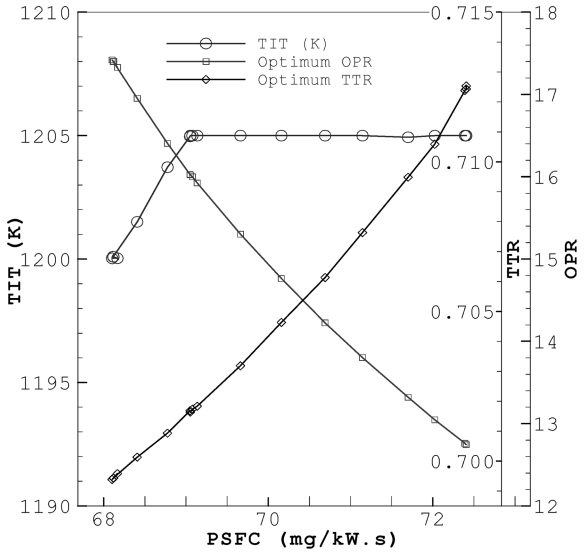

Fig. 10 Optimum cycle parameters for a two-shaft fixed-turbine turboprop.

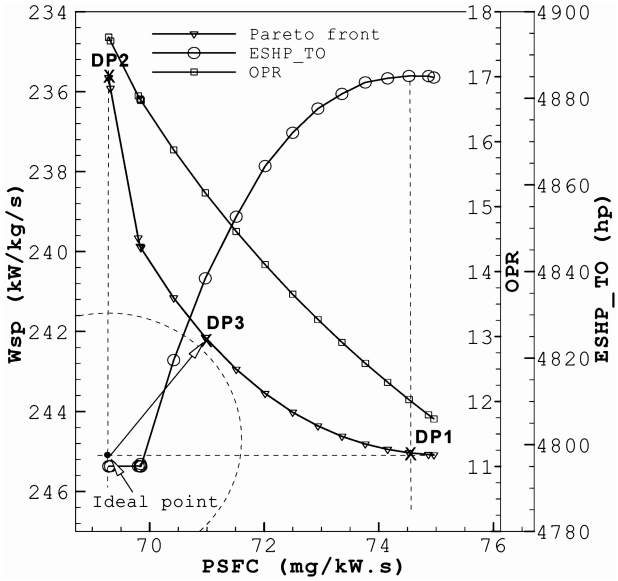

Fig. 9 Tradeoffs surface (Pareto front) for a single-shaft free-turbine turboprop.

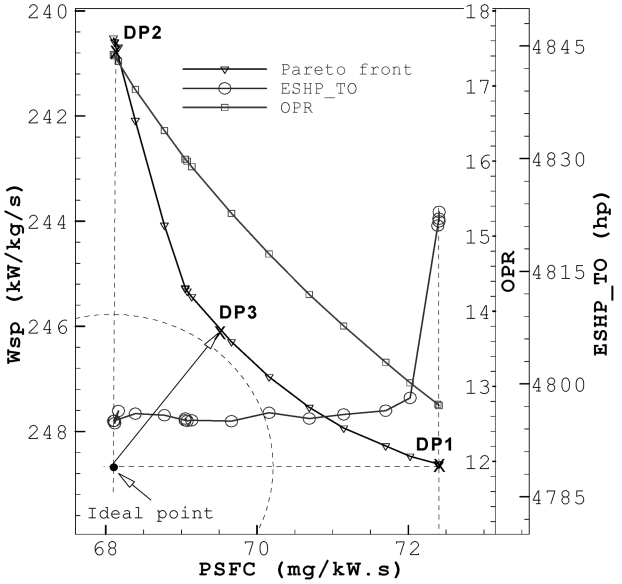

Fig. 11 Tradeoffs surface (Pareto front) for a two-shaft fixed-turbine turboprop.

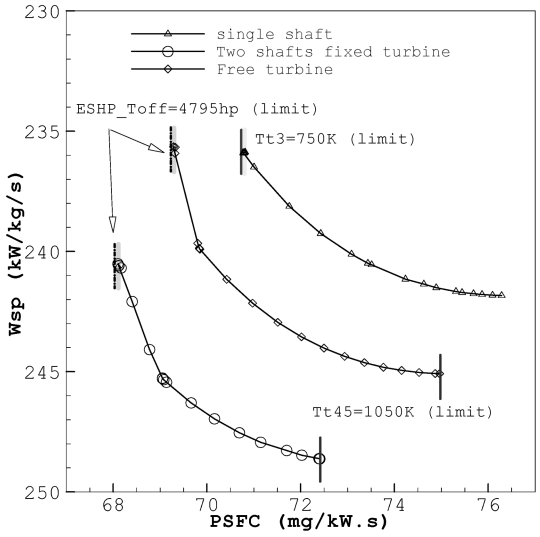

Fig. 12 Comparison of optimal performance.

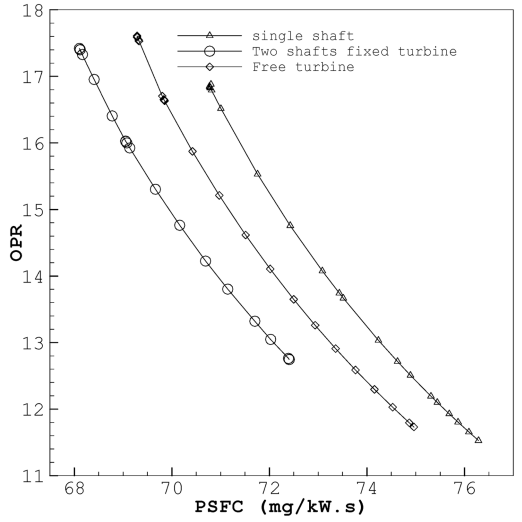

Fig. 13 Comparison of optimum overall pressure ratio.

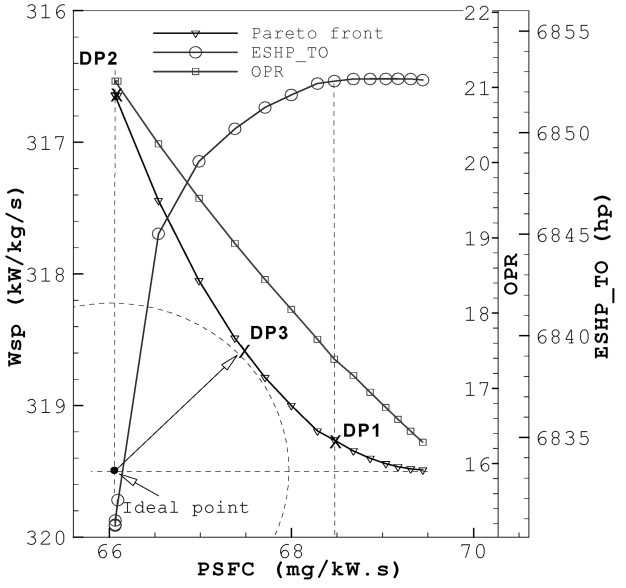

Fig. 14 Tradeoffs surface for a single-shaft fixed-turbine turboprop, advanced technology.

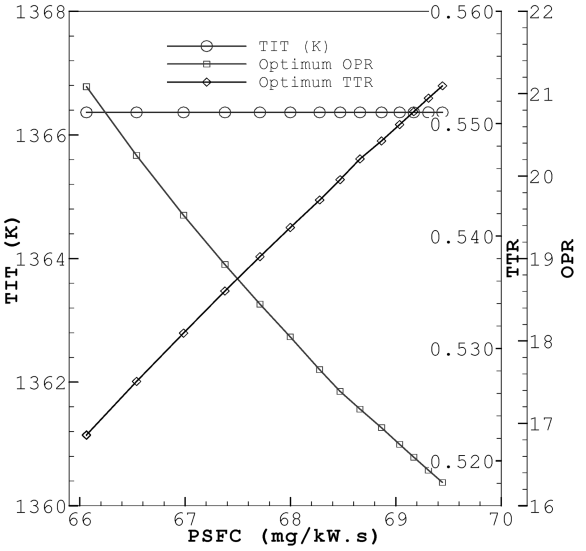

Fig. 15 Optimum cycle parameters for a single-shaft fixed-turbine turboprop, advanced technology.

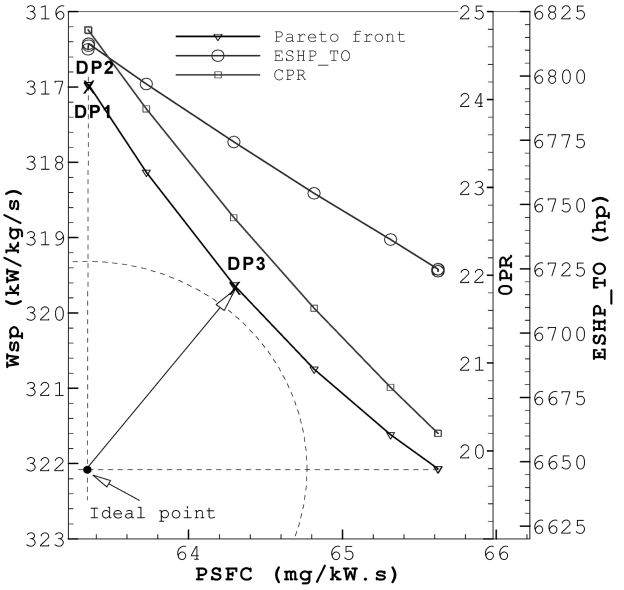

Fig. 16 Tradeoffs surface for a single-shaft free-turbine turboprop, advanced technology.

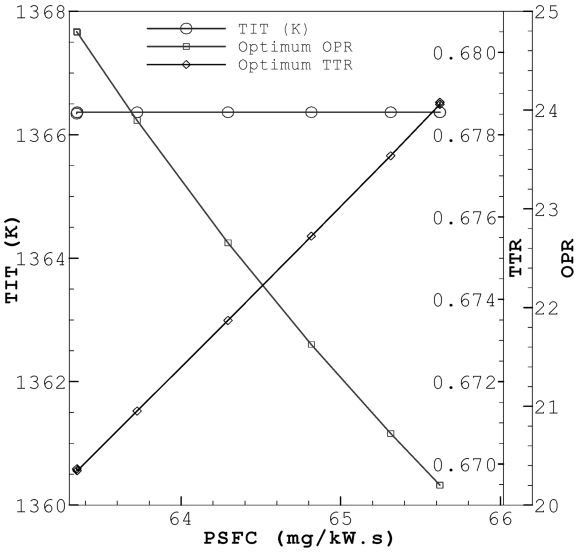

Fig. 17 Optimum cycle parameters for a single-shaft free-turbine turboprop, advanced technology.

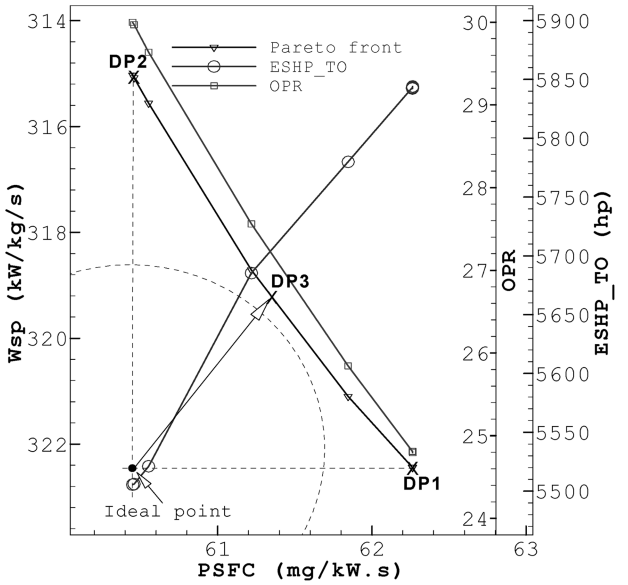

Fig. 18 Tradeoffs surface for the two-shaft fixed-turbine turboprop, advanced technology.

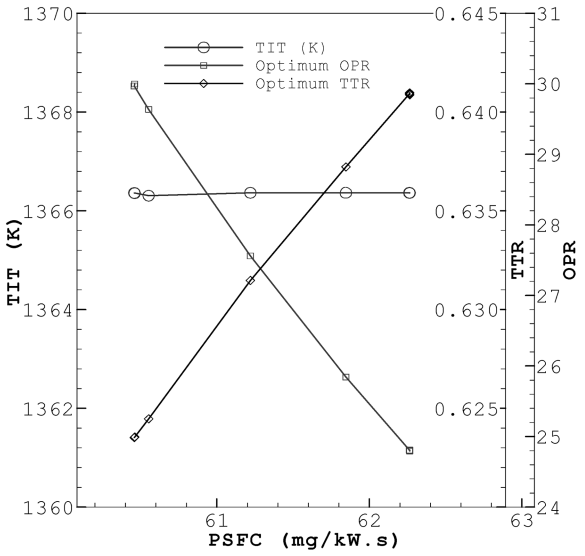

Fig. 19 Optimum cycle parameters two-shaft fixed-turbine turboprop, advanced technology.

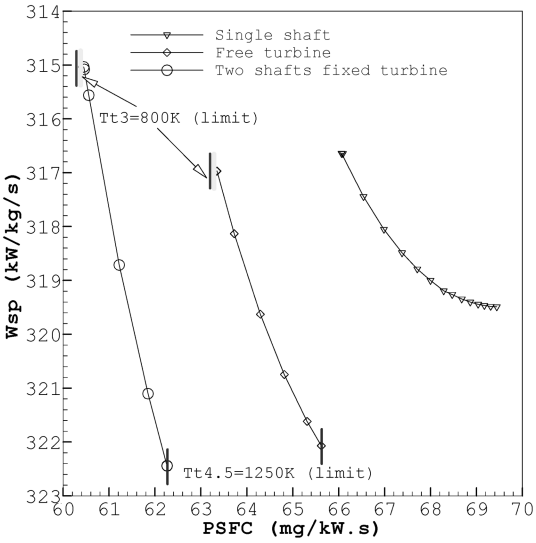

Fig. 20 Comparison of optimal performance, advanced technology.

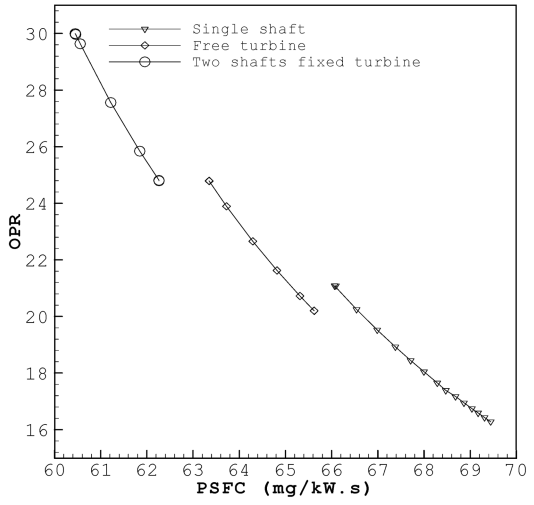

Fig. 21 Comparison of overall pressure ratio, advanced technology.

resulted in a single point, so we decided to enlarge the search space up to 30 to have a wider Pareto front. Another alternative is to use less severe $T_{t4.5}$ constraint by using expensive material or sophisticated cooling. Figures 14–19 illustrate the Pareto fronts and optimum design variables for the three versions of turboprops of advanced technology level. Once more, for all configurations the TIT is at the maximum tolerated value of 1366.4 K, but the optimum overall pressure ratio and turbine temperature expansion rate are varying considerably. All the points on Pareto fronts constitute optimal designs, but the final design points rely on the designer decision. In our case we have proposed three alternative designs: points DP1, DP2 and DP3, as shown by Figs. 14, 16, and 18, which are corresponding to maximum power at takeoff, minimum PSFC, and a compromise, respectively. We can see from Fig. 16 that DP1 and DP2 constitute a unique point for the free-turbine turboprop owing to the

Table 6 Optimum design parameters for an advanced technology level

	Single-shaft fixed turbine			Single-shaft free turbine			Two-shaft fixed turbine		
Design parameters	DP1	DP2	DP3	DP1	DP2	DP3	DP1	DP2	DP3
Compressor pressure ratio	17.39	21.08	18.93	24.79	24.79	22.66	24.81	29.9	27.25
High pressure ratio	——	——	——	——	——	——	15.0	14.95	14.99
Low pressure ratio	——	——	——	——	——	——	1.65	2.0	1.82
Turbine inlet temperature, K	1366.4	1366.4	1366.4	1366.4	1366.4	1366.4	1366.4	1366.4	1366.4
Power turbine temperature ratio	0.5450	0.5223	0.5351	0.6698	0.6698	0.6735	0.6409	0.6239	0.6326
Design performance									
*W*sp, kW/kg/s	319.26	316.64	318.49	316.97	316.97	319.63	322.44	315.03	319.15
PSFC, mg/kW · s	68.47	66.06	67.38	63.35	63.35	64.29	62.26	60.45	61.33
Off-design performance									
Equivalent shaft horsepower at takeoff, hp	6852.54	6831.00	6848.18	6812.02	6812.02	6774.35	5843.26	5567.47	5699.49

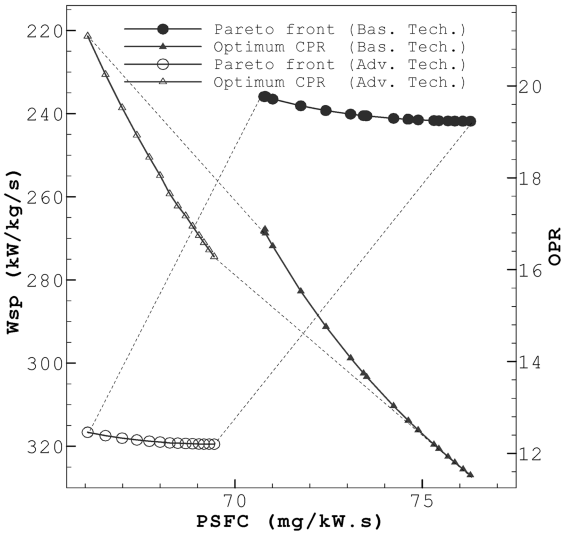

Fig. 22 Technology level influence on optimal design single-shaft fixed-turbine turboprop.

decreasing trend in takeoff-power with PSFC. The compromised design point DP3 nearest to the ideal point is permitting to get a benefit in PSFC and avoid working at the two constraints of temperature. Table 6 gives the optimum cycle parameters and performance corresponding to the proposed design points.

According to previous figures, the takeoff power of 4795 hp did not constitute a strong constraint and the optimization was guided by the constraint of temperature T_{t3} limiting lower values of PSFC and of $T_{t4.5}$ limiting maximum Wsp in the cases of fixed-turbine, free-turbine, and two-shaft fixed-turbine. These limitations are depicted in Fig. 20 showing that the two-shaft fixed-turbine turboprop front offers more design points. It is clear that the two-shaft fixed-turbine is well preferred from fuel economy point of view, but needs high OPRs (Fig. 21) and more LP turbine stages due to higher expansion rates. However, the single-shaft free-turbine configuration presents an intermediate solution vis-à-vis the performance range and other design criteria.

The influence of the technology level on optimal performance and optimum cycle parameters is revealed by Figs. 22–24. By examining the Pareto fronts we can see that the performance is considerably improved with higher technology level and high OPRs are well appreciated.

The optimizations of these variants of turboprops for advanced technology level have led to optimum OPRs laying in between

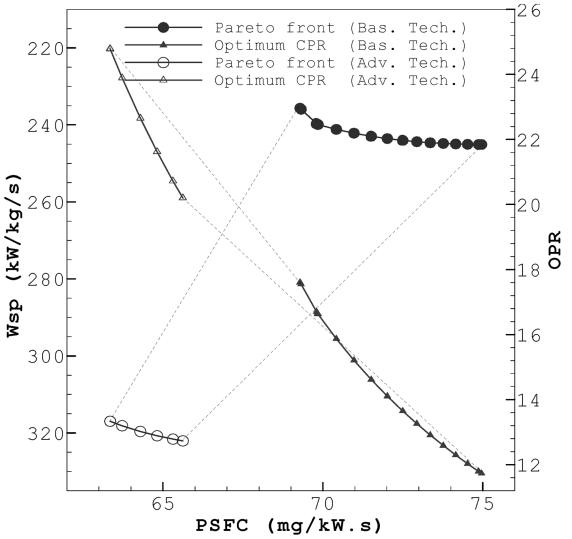

Fig. 23 Technology level influence on optimal design single-shaft free-turbine turboprop.

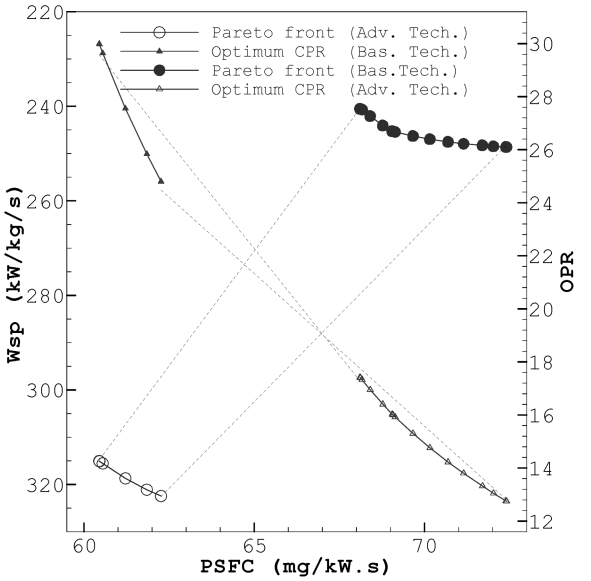

Fig. 24 Technology level influence on optimal design two-shaft fixed-turbine turboprop.

17.39–29.9, resulting in Wsp from 315.03 to 322.44 kW/kg/s and PSFC from 60.45 to 68.47 mg/kW · s. The two-shaft fixed-turbine turboprop seems to perform better, especially with regard to PSFC. However, the free-turbine turboprop offers a compromise (Fig. 21) between the three configurations with regard to OPR and weight.

Finally, the optimizations carried out for the three turboprops' configurations at the same cruising conditions showed that for a basic technology level the two-shaft fixed-turbine turboprop is preferred, owing to better performance for the same OPR range, but needs more LP turbine stages (weight) as compared with the free-turbine version. Also, for an advanced technology the two-shaft fixed-turbine turboprop has quite good performance, but requires higher OPR (weight). The free-turbine turboprop seems to offer an intermediate solution, which is acceptable with regard to performance and other technology criteria.

V. Conclusions

In this study, biobjective optimizations of the propulsion cycles' parameters for three variants of turboprops were carried out based on an efficient optimization algorithm RPSO. The obtained results are illustrating the sensitivity of the engine design to the technology level and constraints. Optimizations of the three turboprops have highlighted how the compressor exit temperature and LP turbine entry temperature were guiding these optimizations. On each Pareto front, three distinguishable design points were selected. However, in view of engine performance and operation limitations, a design near the ideal point offers a good tradeoff. The two-shaft fixed-turbine turboprop is the best performer, but requires higher OPRs, whereas the free-turbine turboprop seems to offer an intermediate solution with regard to other technology criteria. Despite the fact that this present design tool is not based on engine components' operating maps, it has shown capability and versatility when used in early design stages, where the decision taken will determine the course of design process and the final engine performance.

References

[1] Banach, H. J., and Reynolds, C. N., "Turboprop Engine Propulsion for the 1990's," AIAA Paper 81-16848, 1981.

[2] Curry, C. E., and Kron, J., "Aspect of the T56 Power Section Usage/Operating Cost," AIAA Paper 83-1408, 1983.

[3] Treager, I. E., *Aircraft Gas Turbine Technology*, 3rd ed., McGraw–Hill, New York, 1995.

[4] Moris, R. E., "PW100 Evolution of the Design Concept," *Canadian Aeronautics and Space Journal*, Vol. 28, No. , pp. 211–221, 1982.

[5] Brooks, A., and Hirschkron, R., "A Review of Commuter Propulsion Technology," Society of Automotive Engineers Paper 820716, 1982.

[6] Hirschkron, R., and Davis, R. H., "Advanced Turboprop Engines for Long Endurance Naval Patrol Aircraft," American Society of Mechanical Engineers Paper 82-GT-217, 1982.
[7] Saravanamuttoo, H. I. H., "Modern Turboprop Engines," *Aerospace Science and Technology*, Vol. 24, 1987, pp. 225–248, Pergamon Journals Ltd.
[8] Liew, K. H., Urip, E., Yang, S. L., Mattingly, J. D., and Marek, C. J., "Performance (Off-Design) Cycle Analysis for a Turbofan Engine with Interstage Turbine Burner," NASA TM2005-213659.
[9] Mattingly, J. D., *Elements of Gas Turbine Propulsion and Rockets*, AIAA Education Series, 2nd ed., 2006, pp. 87–91, 363–373.
[10] General Motors Allison Division., 501-D22A Operating Manual, SPEC. NO. C787.
[11] Coelho, L., and SierakoWspki, C. A., "A Software Tool for Teaching of Particle Swarm Optimization Fundamentals," *Advances in Engineering Software*, Vol. 39, No. 11, 2008, pp. 877–887. doi:10.1016/j.advengsoft.2008.01.005
[12] Mishra, S. K., "Global Optimization by Particle Swarm Method: A Fortran Program," Munich Personal RePEc Archive Paper No. 874, 2006.
[13] Deb, K., "An Efficient Constraint Handling Method for Genetic Algorithms (2000)," *Computer Methods in Applied Mechanics and Engineering*, Vol. 186, Nos 2–4, 2000, pp. 311–338.
[14] Lockheed Martin, C-130H Hercules Flight Manual, SMP777, Performance Data.
[15] Walsh, P. P., and Fletcher, P., *Gas Turbine Performance*, 2nd ed., Blackwell Science, Boston, 2004, pp. 31–43.
[16] Azarm, S., and Wu, J., "Metric for Quality Assessment of a Multiobjective Design Optimization Solution Set," *Journal of Mechanical Design*, Vol. 123, March 2001, pp. 18–25.
[17] Liu, G. P., Yang, J. B., and Whidborne, J. F., *Multiobjective Optimization and Control*, Research Studies Press Ltd., Baldock, United Kingdom, 2003.
[18] Augustine, R. Dovi, and Gregory, A. Wrenn, "Aircraft Design for Mission Performance Using Nonlinear Multiobjective Optimization Methods," NASA Contractor Rept. CR4328, Oct. 1990.
[19] Kong, C., and Chung, S., "Performance Simulation of a Turboprop Engine for Basic Trainer," *KSME International Journal*, Vol. 16, No. 6, 2002, pp. 839–850.

A. Prasad
Associate Editor